Microgrids Frequency Control Considerations within the Framework of the Optimal Generation Scheduling Problem

Amir H. Hajimiragha, *Senior Member, IEEE,* Mohammad R. Dadash Zadeh, *Senior Member, IEEE,* and Somayeh Moazeni, *Member, IEEE*

***Abstract*—Microgrids are perceived to play an important role in the future of smart grids. Cost reduction and frequency regulation are among the major concerns in this context. This paper aims to study the mutual impacts of these issues and to propose an integrated mathematical framework in order to achieve minimum costs while maintaining frequency-regulation requirements. Inspired by the operational practices and requisites of the real-world microgrid applications, different methods of frequency control are reviewed and discussed. This is followed by developing adequate models for the different types of frequency-regulation mechanisms in the framework of the microgrid generation scheduling problem. The application of the proposed methodology to the Bella Coola microgrid in British Columbia, Canada, is explained, and several numerical results are presented and discussed.**

***Index Terms*—Droop, frequency control, generation scheduling, isochronous, microgrid, reserve margin.**

NOMENCLATURE

Abbreviations

AMPL	A modeling language for mathematical programming.
CHP	Combined heat and power.
ECS	Electronically coupled source.
ILS	Isochronous load sharing.
MILP	Mixed integer linear programming.
MINLP	Mixed integer nonlinear programming.
MDT	Minimum down time.
MUT	Minimum up time.

Indices

i, j	Index for load or a microgrid asset.
t	Index for time steps.

Manuscript received November 20, 2013; revised June 8, 2014 and September 27, 2014; accepted November 16, 2014. Date of publication December 18, 2014; date of current version February 16, 2015. Paper no. TSG-00861-2013.

A. H. Hajimiragha is with GE Digital Energy, GridIQ Innovation Center, Markham, ON L6C 0M1, Canada (e-mail: amir.hajimiragha@ge.com).

M. R. Dadash Zadeh is with the Department of Electrical and Computer Engineering, Western University, London, ON N6A 5B9, Canada (e-mail: mdadash@uwo.ca).

S. Moazeni is with the School of Systems and Enterprises, Financial Engineering, Stevens Institute of Technology, Hoboken, NJ 07030 USA (e-mail: smoazeni@stevens.edu).

Color versions of one or more of the figures in this paper are available online at http://ieeexplore.ieee.org.

Digital Object Identifier 10.1109/TSG.2014.2375251

Sets

$\mathcal{D}$	Set of dispatchable gensets.
$\mathcal{I}$	Set of dispatchable gensets running in ILS mode.
$\mathcal{K}_1, \ldots, \mathcal{K}_4$	Subsets of $\mathcal{T}$.
$\mathcal{L}$	Set of loads.
$\mathcal{R}$	Set of renewable power sources.
$\mathcal{S}$	Set of storage devices.
$\mathcal{T}$	Set of time steps in the multi-interval generation scheduling problem.
$\mathcal{T}^*$	Set of time steps excluding the first step.

Parameters

$C^R_{i,t}$	Renewable capability (−).
$C^{sys,slack}_t$	Penalty factor for microgrid system slack variable (\$/kWh).
$C^{S,CHG}_i$	Penalty factor for storage charging (\$/kWh).
$C^{S,DHG}_i$	Penalty factor for storage discharging (\$/kWh).
$C^{S,slack}_i$	Penalty factor for SOC slack variable (\$/kWh).
Cf^D_i	Fuel cost of dispatchable genset i (\$/liter).
$Cop^{S,CHG}_i$	Operating cost of storage charging (e.g., electrolyzer) (\$/kWh).
$Cop^{S,DHG}_i$	Operating cost of storage discharging (e.g., fuel cell) (\$/kWh).
Csh^D_i	Shut-down cost of dispatchable genset i (\$).
Cst^D_i	Start-up cost of dispatchable genset i (\$).
$Cst^{S,CHG}_i$	Start-up cost of storage charging (e.g., electrolyzer) (\$).
$Cst^{S,DHG}_i$	Start-up cost of storage discharging (e.g., fuel cell) (\$).
$I^{S,CHG}_{i,t}$	Incentive for storage charging (\$/kWh).
K^D_{1i}	Constant parameter corresponding to fuel consumption of dispatchable i (kg/h).
K^D_{2i}	Constant parameter corresponding to fuel consumption of dispatchable i (kg/kWh).
LF^D_i	Load factor of dispatchable genset i (−).
MUT^D_i	Dispatchable minimum up-time (hour).
MDT^D_i	Dispatchable minimum down-time (hour).

$MUT_i^{S,CHG}$ Storage charging (e.g., electrolyzer) minimum up-time (hour).
$MDT_i^{S,CHG}$ Storage charging minimum down-time (hour).
P_i^L Load power (kW).
$P_{i,t}^{Rf}$ Renewable forecasted power (kW).
$P_i^{S,loss}$ Storage dissipation or stand-by loss (kWh/h).
$P_{min,i}^{S,CHG}$ Lower bound of storage charging power (kW).
$P_{max,i}^{S,CHG}$ Upper bound of storage charging power (kW).
$P_{min,i}^{S,DHG}$ Lower bound of storage discharging power (kW).
$P_{max,i}^{S,DHG}$ Upper bound of storage discharging power (kW).
$P_{min,i}^{D}$ Minimum acceptable operating power of dispatchable genset i (kW).
$P_{rated,i}^{G}$ Nameplate power rating of a general genset (kW).
$P_{rated,i}^{D}$ Nameplate power rating of dispatchable genset i (kW).
RD_i^D Maximum rate of generation decrease for dispatchable genset i (kW/h).
RU_i^D Maximum rate of generation increase for a dispatchable genset i (kW/h).
$RM_{req,t}^{+}$ Required positive reserve margin (kW).
$RM_{req,t}^{-}$ Required negative reserve margin (kW).
$RM_{act,t}^{+}$ Actual positive reserve margin (kW).
$RM_{act,t}^{-}$ Actual negative reserve margin (kW).
r^+, r^-,u^+,u^- Small positive numbers (−).
$SOC_{init,i}^S$ Initial state of charge (SOC) (kWh).
$SOC_{max,i}^S$ Upper bound of storage SOC (kWh).
$SOC_{min,i}^S$ Lower bound of storage SOC (kWh).
ΔT Dispatch time (hour).
η_i^D Efficiency of dispatchable genset i (kWh/kg).
$\eta_{min,i}^D$ Efficiency of dispatchable genset i at minimum acceptable operating power (kWh/kg).
$\eta_{rated,i}^D$ Efficiency of dispatchable genset i at nameplate rating power (kWh/kg).
$\eta_i^{S,CHG}$ Storage charging efficiency (−).
$\eta_i^{S,DHG}$ Storage discharging efficiency (−).
ρf_i^D Fuel density of dispatchable genset i (kg/liter).

Variables

$b_{i,t}^D$ Binary variable for dispatchable i representing the online/offline status at time step t (−).
$b_{i,t}^{S,CHG}$ Binary variable for storage charging representing the online/offline status at time step t (−).
$b_{i,t}^{S,DHG}$ Binary variable for storage discharging representing the online/offline status at time step t (−).
$F_{i,t}^D$ Fuel consumption rate of dispatchable genset i at time step t (kg/h).
k Equal share of generation units running in ILS mode (−).
$OF_{i,t}^D$ Dispatchables cost term in the objective function ($).
$OF_{i,t}^S$ Storage devices cost term in the objective function ($).
P_i^G Power generation contribution of a general genset (kW).
$P_{i,t}^D$ Generated power of dispatchable genset i at time step t (kW).
$P_{i,t}^R$ Power generation of renewable source i at time step t (kW).
$P_{i,t}^{S,CHG}$ Storage charging power (kW).
$P_{i,t}^{S,DHG}$ Storage discharging power (kW).
$P_t^{sys,slack}$ Microgrid system slack variable at time step t (kW).
$SOC_{i,t}^S$ Storage SOC at time step t (kWh).
$SOC_{i,t}^{S,slack}$ Storage slack variable representing the violation from $SOC_{min,i}^S$ at time step t (kWh).
$V_{i,t}^D$ Auxiliary continuous variable for dispatchable genset i running in ILS mode at time step t (kW).
$W_{i,j,t}^D$ Auxiliary continuous variable for dispatchable gensets i and j running in ILS mode at time step t (kW).
$\alpha_i^{S,CHG}$ Non-negative variable for storage device i limiting the rate of change of charging power (kW).
$\beta_i^{S,DHG}$ Non-negative variable for storage device i limiting the rate of change of discharging power (kW).
$\delta_{i,t}^{D,st}$ Auxiliary binary variable for dispatchable genset i representing the transition from offline to online at time step t (−).
$\delta_{i,t}^{D,sh}$ Auxiliary binary variable for dispatchable genset i representing the transition from online to offline at time step t (−).
$\delta_{i,t}^{S,CHG}$ Auxiliary binary variable for storage charging representing the transition from offline to online at time step t (−).
$\delta_{i,t}^{S,DHG}$ Auxiliary binary variable for storage discharging representing the transition from offline to online at time step t (−).

I. Introduction

A. Motivation

MICROGRIDS are commonly referred to as self-sustained small distribution systems composed of loads and multiple generation and/or storage assets. Microgrids can offer greater availability and flexibility through multiple sources of power generation and/or storage and immunity from the fault conditions or power disturbances in the upstream grid [1], [2]. Buying, storing, and selling energy

in different time frames as well as providing ancillary services for the grid are some opportunities that can bring about economic justification for the microgrids. Microgrids present higher levels of reliability especially for the critical loads such as hospitals, military bases, and data centers in view of the existing threats imposed by natural disasters and terrorist attacks. This level of security and new economic opportunities especially in remote communities where there is no access to transmission and distribution grid [3], together with their role in future smart grids [4], demonstrate the unique value and importance of microgrids. Frequency regulation and operation cost reduction are among the major concerns in microgrid applications. Therefore, appropriate methods and/or analytical tools are required to address them.

B. Literature Review and Methodology

Frequency regulation and cost reduction in a microgrid are typically discussed in different time frames. Thus, frequency regulation is associated with a very short time scale (e.g., from a fraction of a second to a couple of seconds) while cost reduction, which is realized by optimal dispatching of generation and storage devices, is usually evaluated in a time span of several hours. This may suggest different frameworks to study these concepts, especially by considering the fact that frequency regulation is often addressed in a lower level of control. However, despite the different time frames or control levels through which these issues are analyzed, the source/type of frequency regulation does influence the result of the microgrid generation scheduling. Thus, the generation/storage units that are responsible for maintaining the frequency in an islanded microgrid provide reserve power margins in the microgrid. These reserve margins directly determine the lower and upper bounds of power for that unit in the generation scheduling problem. Therefore, power generation constraints of the frequency regulator should be reflected in the microgrid generation scheduling algorithm.

The aforementioned reserve power in the bulk grid is commonly referred to as spinning reserve in the literature. Spinning reserve is basically the extra generation capacity that is available within a short period of time to compensate for unexpected events such as sudden load changes or power plants outages. Moreover, the issue of reserve power has become critically important in generation scheduling for the grids with a high penetration of intermittent renewable power sources where a mismatch is experienced between the renewable forecasts used in the day-ahead unit commitment and the renewable power in real-time dispatch [5], [6]. In this regard, reserve power requirements/constraints are essential in the power systems unit commitment, optimal dispatch, or generation scheduling problems; this issue is widely studied and reported (see [7]–[10]). The application of the similar reserve power concept to microgrids has also been reported (see [11], [12]). This issue becomes even more critical in microgrids due to their relatively low level of inertia and dominancy of renewable power share compared to the bulk grid.

There are several studies in the area of microgrid generation scheduling, each of which considers particular types of assets and constraints (e.g., see [13]–[17]). In particular, reserve power requirements in these studies are either neglected or simply considered as a few percent of the total load and/or renewable power sources. For example in [18], the spinning reserve requirement is reflected as the decrease in the maximum limit and the increase in the minimum limit of the first generator in a control area. A somewhat similar approach to capture the microgrids spinning reserve requirements is used in [19]. The contribution of upstream grid in covering the spinning reserve requirement has also been considered in [20].

Depending on the type of assets in a microgrid that is whether there are generators with inertia in the rotating masses (e.g., diesel/wind gensets and CHP units) or electronically-coupled sources (e.g., battery, solar, or fuel cell), different frequency control mechanisms are applied. Thus, in practical microgrid applications, frequency can be regulated by either a single/multiple units equipped with isochronous speed controls or bidirectional power conversion systems. Provision of reserve power in the microgrid based on these methods requires developing particular types of constraints in the microgrid generation scheduling problem. Therefore, the frequency regulating source in a microgrid should be appropriately modeled in the framework of the generation scheduling problem; this has not been adequately addressed in the previous contributions in this area.

C. Objectives and Contributions

Motivated by the existing and growing interest in microgrids and the vital need for their economic and reliable operation, this paper aims to incorporate the frequency-control requirements into the microgrid's generation scheduling framework. In particular, this paper presents the following new contributions.

1) Inspired by real-world microgrid projects and the operational limitations experienced in practice, a comprehensive microgrid generation scheduling problem based on a rolling time horizon is developed. This formulation considers three major types of assets (i.e., dispatchables, renewables, and storage devices) with their corresponding operational constraints with a particular emphasis on the microgrid reserve power requirements.
2) Depending on the microgrid conditions and in order to accommodate considerable load variations and/or significant renewable penetration, multiple isochronous machines or storage devices equipped with bidirectional power conversion systems can be responsible for regulating the frequency. These machines/devices simultaneously raise or lower their power generation to maintain the desired frequency. This operation mode is referred to as isocronous load sharing (ILS). This paper aims to incorporate the defining characteristics of this mode into the microgrid generation scheduling problem.
3) Particular types of renewable power sources such as run-of-the-river hydro units with reservoir represent a lower level of intermittency; therefore, they can be operated as isochronous machines during certain times.

An appropriate procedure is also proposed to support the isochronous operation of a renewable power source within the microgrid generation scheduling problem.

The remainder of this paper is structured as follows. Section II discusses different frequency control mechanisms in microgrids that are inspired by real-world applications. Section III presents general methodology of a microgrid optimal generation scheduling problem. Section IV describes the mathematical models of the microgrid's devices and operation, and the formulation of the optimization problem. The proposed enhancements to the microgrid generation scheduling problem which account for the reserve margin requirements are comprehensively discussed in Section V. The description of a real-world microgrid example (i.e., Bella Coola in British Columbia, Canada) is presented in Section VI. This is followed by a numerical illustration in Section VII. Finally, Section VIII summarizes the main conclusions of this paper.

II. Microgrid Frequency Control

In grid-connected microgrids, any immediate change in the load and renewable powers is compensated by the grid. Therefore, the grid itself performs as a frequency-regulating source. When no connection to the grid exists different solutions are applied in real-world microgrid applications, depending on the type of generation resources and load variation profile. These solutions are briefly outlined below.

A. Single Unit With Isochronous Speed Control

In this mode of operation, one dispatchable source adjusts the frequency by isochronous speed control while the remaining sources contribute in droop speed control mode. For an ac generator set (genset) with isochronous speed control, the governor senses any changes in the frequency, and it quickly raises/reduces the energy applied to the prime mover in order to maintain a fixed frequency (50/60 Hz) [21].

Fast response of isochronous speed control to transient load changes in a microgrid ensures that frequency is controlled within a tight range (e.g., $\pm$ 0.25% deviation), even when load or renewable changes are substantial or the changes happen at a fast rate. However, note that the control mechanism (i.e., isochronous or droop) is not the only influential factor. Thus, the accuracy of the frequency regulation in isochronous mode also depends upon the size and type of the synchronous machine. For example, a small-size natural gas generator (e.g., in the range of 20–30 kW) usually represents lower performance compared to a same size diesel generator due to the differences in fueling and/or combustion mechanisms. As well, a diesel generator may regulate the frequency in a tighter range compared to a hydro generator when they operate in isochronous speed control mode [22]. This issue is considered for making decision on the type of isochronous source in islanded microgrids, depending on the load level and the nature of changes (e.g., slow/fast). It is also important to note that the isochronous machine is not under the direct control of the central microgrid control or energy management system. It should be running independently to quickly catch the power swings in the microgrid. However, its steady-state power contribution can be impacted by other *non-isochronous* generation or storage devices in the microgrid. Therefore, the optimal generation scheduling problem solved by the microgrid control or energy management system can indirectly change the steady-state power generation of the isochronous machine.

B. ILS Control

In this mode of operation, a combination of dispatchable gensets, which mostly reside in close proximity to one another, maintains the load-generation balance. This mode of operation is appropriate when load variation is substantial so that a single dispatchable with isochronous speed control cannot regulate the frequency.

In this mode, all gensets in the microgrid assume an equal percentage of their full-load capacity. The purpose of this mode is to proportionally divide a common load between multiple gensets while maintaining a fixed frequency on an islanded microgrid [21], [23]. In this mode, each machine has its own isochronous speed control function but an additional signal for each machine causes the fuel rate to slightly increase or decrease to ensure load sharing with other gensets happens at the same percent (k) of generator's full-load capacity. In order to implement this scheme, individual gensets are connected by load sharing lines by which loading on each machine can be communicated with other isochronous machines in the microgrid. This information is used by each machine to provide a correction signal so that all machines can share the same percentage of their full-load capacity. The key to the implementation of this control scheme is the communication of load sharing data between individual isochronous machines; otherwise, the isochronous machines will "fight" with each other and cause the system to become unstable. Based on the aforementioned theory of operation, the following mathematical equations can be developed for an islanded microgrid composed of n gensets running in ILS mode:

$$\sum_{i=1}^{n} P_i^G = \sum_{i=1}^{n} kP_{rated,i}^G = \sum_{i\in\mathcal{L}} P_i^L \tag{1}$$

$$k = \frac{P_1^G}{P_{rated,1}^G} = \frac{P_2^G}{P_{rated,2}^G} = \cdots = \frac{\sum_{i=1}^{n} P_i^G}{\sum_{i=1}^{n} P_{rated,i}^G}. \tag{2}$$

It is also important to note that the main reason for having the generation units of ILS scheme operate in close proximity to each other is to guarantee a reliable communication.

C. Electronically Coupled Sources (ECSs) Control

Current control mode has been widely applied to electronic power converters to interface renewable and stored energies to the electric grid [24]. In current control mode, an ECS behaves like a variable current controlled source. The magnitude and angle of the current can be adjusted to achieve certain control set-points, such as voltage level, active power, or frequency depending on the source type and control strategy. If one ECS, such as an energy storage, is set to control

the microgrid generation-load balance, the ECS adjusts its current to maintain the voltage magnitude [25]. In this mode, the frequency remains at a nominal level since ECS generates current with nominal frequency regardless of voltage magnitude. However, any load-generation imbalance impacts the voltage magnitude, and is immediately compensated by ECS.

If several ECSs are set to control the microgrid generation-load balance, the controllers of ECSs must be coordinated to ensure system stability in all required conditions [26]. One of the simplest and most effective approaches for coordinating controllers is to allow the frequency of ECS current to vary, and apply the concepts of isochronous and droop control for load sharing purpose. This can be implemented by employing an additional control layer which uses measured frequency to offset the ECS output current on top of conventional current control mode [24]. In this control strategy, each ECS controller synchronizes itself to the point of coupling by using a phase-locked loop. In addition, the output power, and thereby the output current, is drooped by the frequency variation [25]. In this control strategy, all the ECSs are in droop mode, so steady state error in frequency control is expected. This is similar to the case when several synchronous machines with droop speed control fail to regulate the frequency unless load/renewable changes are low or they happen at a slow rate. However, if one ECS is set to operate in isochronous mode while the rest of ECSs are operated in droop mode, the frequency will stabilize at a nominal level after any load/generation change. That is all provided that the ECS operating in isochronous mode is large enough to be capable of generating/absorbing the entire change in load or generation.

III. Microgrid Generation Scheduling

Cost reduction is a major concern for microgrid installations. In particular, this is of great importance for the remote communities, which are heavily dependent on diesel-based power generation [3]. Depending on the microgrid application, a wide variety of generation and storage devices may exist with different start-up/shut-down costs as well as fuel consumption rates or efficiencies. Moreover, there are plenty of operational limitations specific to each asset. In view of all these considerations and limitations, making decisions on how to control the microgrid to achieve minimum cost is a challenging task that should be resolved through an optimization process; this is referred to as microgrid generation scheduling, which can be embedded in a microgrid energy management or supervisory control system.

Since optimal decisions are made for the present and future time (i.e., *prediction horizon*), the microgrid generation scheduling problem is a multi-interval optimization problem. Decisions are also updated by rerunning the optimization calculations every few minutes/hours (i.e., *dispatch time*) to account for the time-varying nature of loads and renewable power sources. Prediction horizon and dispatch time determine the total number of time steps (i.e., *prediction length*) in the microgrid optimization problem. Fig. 1 illustrates this concept for a 24-h prediction horizon and a 12-min dispatch time which result in a 120-step prediction length. The aforementioned method is commonly referred to as rolling time horizon or model predictive control [27], [28].

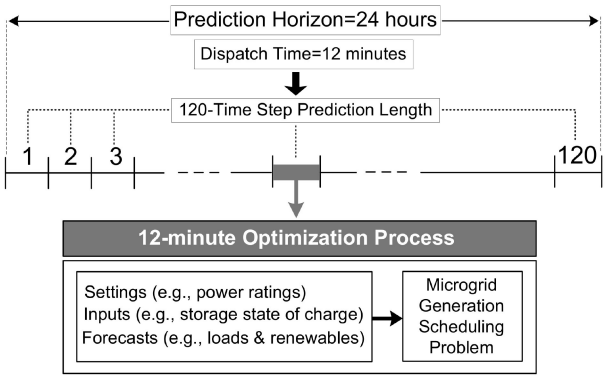

Fig. 1. Demonstration of the multi-interval microgrid generation scheduling problem.

The optimization framework cited earlier should take into account the different types and number of assets in the microgrid with their corresponding operational limitations and constraints such as lower and upper bounds of powers and charge states, ramp rates, and minimum up and down times. In order to model some of these operational considerations in the optimization problem, discrete (integer/binary) variables and complex constraints need to be defined; this results in MILP/MINLP formulations. Due to the real-time requirement of the microgrid generation scheduling problem and its inherent computational challenges, it is preferable to keep the model linear.

IV. Mathematical Formulation

This section represents different terms of objective function as well as the constraints of a microgrid optimal generation scheduling problem without considering the reserve power requirements. Also, since this paper is mainly focused on the ILS scheme where generation units should operate in close proximity to each other, grid model and its corresponding nonlinear power flow constraints are not considered in this model.

A. Dispatchables Cost

In order to reduce the computational burden of the generation scheduling problem, the fuel consumption rate of dispatchable gensets is assumed to be an affine function of their generated power as expressed below

$$F^D_{i,t} = K^D_{1i} + K^D_{2i} P^D_{i,t}. \tag{3}$$

While (3) is accurate enough for practical applications, more sophisticated nonlinear expressions can be considered as long as they can be linearized to keep the model as an MILP problem. Also, K^D_{1i} and K^D_{2i} can be calculated based on the parameters of a dispatchable genset at minimum and rated power levels. Thus, the efficiency of a dispatchable genset is defined as the ratio of its generated power to the rate of fuel

consumption in terms of kWh/kg as expressed below

$$\eta_i^D = \frac{P_i^D}{F_i^D}. \tag{4}$$

Combining (3) and (4) enables to express the efficiency of dispatchable i as a function of its generated power

$$\eta_i^D = \frac{P_i^D}{K_{1i}^D + K_{2i}^D P_i^D}. \tag{5}$$

Since efficiencies of dispatchables are known at minimum and rated power levels ($P_{min,i}^D$, $P_{rated,i}^D$), it is possible to determine K_{1i}^D and K_{2i}^D in terms of the information of the minimum and rated points; i.e., ($P_{min,i}^D$, $\eta_{min,i}^D$) and ($P_{rated,i}^D$, $\eta_{rated,i}^D$). Plugging these two points in (5) and solving for K_{1i}^D and K_{2i}^D results in the following general expressions:

$$K_{1i}^D = \frac{P_{rated,i}^D . P_{min,i}^D}{P_{rated,i}^D - P_{min,i}^D} \left(\frac{1}{\eta_{min,i}^D} - \frac{1}{\eta_{rated,i}^D} \right) \tag{6}$$

$$K_{2i}^D = \frac{1}{P_{rated,i}^D - P_{min,i}^D} \left(\frac{P_{rated,i}^D}{\eta_{rated,i}^D} - \frac{P_{min,i}^D}{\eta_{min,i}^D} \right). \tag{7}$$

Based on (3) and by knowing the fuel cost and density, it is possible to calculate the operation cost of dispatchable i in terms of \$/h. Hence, the following expression represents the dispatchable's-related cost in time step t in terms of \$ in the objective function:

$$OF_{i,t}^D = \left(K_{1i}^D + K_{2i}^D P_{i,t}^D\right) . \frac{Cf_i^D}{\rho f_i^D} . \Delta T + Cst_i^D . \delta_{i,t}^{D,st} + Csh_i^D . \delta_{i,t}^{D,sh}. \tag{8}$$

B. Storage Devices Cost

The storage device's-related cost in the objective function including operation and start-up costs can be formulated as follows:

$$OF_{i,t}^S = \left(Cop_i^{S,CHG} . P_{i,t}^{S,CHG} + Cop_i^{S,DHG} . P_{i,t}^{S,DHG}\right) . \Delta T + Cst_i^{S,CHG} . \delta_{i,t}^{S,CHG} + Cst_i^{S,DHG} . \delta_{i,t}^{S,DHG}. \tag{9}$$

Note that for a hydrogen storage system, $P_{i,t}^{S,CHG}$ and $P_{i,t}^{S,DHG}$ are interpreted as electrolyzer input power and fuel cell output power, respectively. Also, shut-down cost of storage devices has been disregarded here; however, a procedure similar to the one for dispatchables can be adopted to factor this cost in the objective function.

C. Objective Function

The model's objective is to minimize the microgrid total cost. This includes start-up and operation costs of dispatchables and storage devices as developed in previous sections. Note that the operation cost of renewable power sources is disregarded. Therefore, the following objective function for the microgrid generation scheduling problem is considered:

$$min \sum_{t \in \mathcal{T}} \left(\sum_{i \in \mathcal{D}} OF_{i,t}^D + \sum_{i \in \mathcal{S}} OF_{i,t}^S \right) \tag{10}$$

where $\mathcal{T} = \{1, \ldots, \text{prediction length}\}$. Note that depending on the microgrid conditions and configurations and in order to support some features or to achieve desired performance, additional cost or incentive terms can be added to the objective function. These terms are related to, but not limited to, promoting storage charging, smooth operation of storage devices, permitted violation from the storage minimum acceptable charge, or support of isochronous operation of a low-intermittent renewable power source. These terms are further discussed in the following sections. Also, for grid-connected microgrids, appropriate terms can be added to the objective function to reflect the cost of buying and revenue from selling to the grid. Moreover, the presented formulation can be slightly updated to suit microgrids with more than one single energy carrier.

D. Constraints

1) Power Balance: Generation-load balance in the microgrid generation scheduling problem for a single energy carrier (e.g., electricity) is respected by the following constraint:

$$\sum_{i \in \mathcal{R}} P_{i,t}^R + \sum_{i \in \mathcal{D}} P_{i,t}^D + \sum_{i \in \mathcal{S}} \left(P_{i,t}^{S,DHG} - P_{i,t}^{S,CHG} \right) - \sum_{i \in \mathcal{L}} P_{i,t}^L = 0. \quad \forall t \in \mathcal{T} \tag{11}$$

2) Dispatchables Power:

$$b_{i,t}^D . P_{min,i}^D \leq P_{i,t}^D \leq b_{i,t}^D . P_{rated,i}^D \quad \forall i \in \mathcal{D} \wedge t \in \mathcal{T} \tag{12}$$

where $b_{i,t}^D = 1$ represents the online status of dispatchable i at time step t. This constraint ensures that if power contribution of dispatchable i is needed at time step t, its value is not below or above certain limits.

3) Dispatchables Loading Factor: Although the calibration of the non-isochronous, isochronous, and ILS control systems is based on nameplate rating power and as such can operate through any loading conditions, dispatchable gensets wear out faster when operated at high percentage of load. Therefore, particular operational considerations should be in place for different applications, such as prime power, emergency, standby or back up to ensure high reliability and longer life cycles. Since the context of discussion in this paper is an isolated microgrid, prime power application is particularly considered. In this application, a dispatchable genset is capable of running continuously while supplying a variable load when operated for an unlimited number of hours per year. According to ISO 8528-1, a prime power dispatchable genset can provide the full nameplate rating for a period of time but the genset's average output power over 24 h of operation should not exceed 70% of the nameplate rating (i.e., 70% load factor). This does not include the genset's non-running time. The aforementioned operational constraint can be mathematically expressed as follows:

$$\sum_{t \in \mathcal{T}} P_{i,t}^D \leq LF_i^D . P_{rated,i}^D . \sum_{t \in \mathcal{T}} b_{i,t}^D \quad \forall i \in \mathcal{D}. \tag{13}$$

It is worth mentioning that a 10% overload in accordance with ISO 3046-1 is disregarded in this paper since it is limited to the brief time of 25 h per year.

4) Dispatchables Ramping Up and Down:

$$P^D_{i,t} - P^D_{i,t-1} \le RU^D_i.\Delta T$$
$$P^D_{i,t-1} - P^D_{i,t} \le RD^D_i.\Delta T \quad \forall i \in \mathcal{D} \wedge t \in \mathcal{T}. \tag{14}$$

It is important to note that in microgrid applications as opposed to the bulk grid, the aforementioned requirements on generators' load pick-up and drop-off can be covered by the corresponding local controllers. Also, ramp rate constraints are relaxed for ILS units. This is due to the fast-response requirements of these units to quickly address the swings in loads and renewable power sources. Interested readers are also referred to [9], [29], and [30] for an alternative formulation for ramping constraints that is mostly applicable to large thermal power plants where power trajectories during start-up and shut-down processes should be enforced.

5) Dispatchables Start-Up:

$$\delta^{D,st}_{i,t} - b^D_{i,t} + b^D_{i,t-1} \ge 0 \quad \forall i \in \mathcal{D} \wedge t \in \mathcal{T}. \tag{15}$$

This constraint enforces $\delta^{D,st}_{i,t} = 1$ following the transition of dispatchable i from offline to online in two consecutive time steps.

6) Dispatchables Shut-Down:

$$\delta^{D,sh}_{i,t} - b^D_{i,t-1} + b^D_{i,t} \ge 0 \quad \forall i \in \mathcal{D} \wedge t \in \mathcal{T}. \tag{16}$$

This constraint enforces $\delta^{D,sh}_{i,t} = 1$ following the transition of dispatchable i from online to offline in two consecutive time steps.

7) Dispatchables Minimum Up Time:

$$b^D_{i,t} - b^D_{i,t-1} - b^D_{i,k} \le 0 \quad \forall i \in \mathcal{D} \wedge t \in \mathcal{T}^* \wedge k \in \mathcal{K}_1 \tag{17}$$

where

$\mathcal{K}_1 = \{t, \ldots, min(t + 10 \times MUT^D_i - 1, \text{prediction length})\}$. This constraint ensures that if a dispatchable is set online, it will continue running for a certain period of time [31].

8) Dispatchables Minimum Down Time:

$$b^D_{i,t-1} - b^D_{i,t} + b^D_{i,k} \le 1 \quad \forall i \in \mathcal{D} \wedge t \in \mathcal{T}^* \wedge k \in \mathcal{K}_2 \tag{18}$$

where

$\mathcal{K}_2 = \{t, \ldots, min(t+10\times MDT^D_i - 1, \text{prediction length})\}$. This constraint precludes start-up a dispatchable short after receiving a stop command [31]. Interested readers are also referred to [9] for an alternative formulation to enforce minimum up and down times requirements.

9) Renewables Power:

$$P^R_{i,t} = P^{R_f}_{i,t} \quad \forall i \in \mathcal{R} \wedge t \in \mathcal{T}. \tag{19}$$

This constraint ensures that only the forecasted values of renewable power sources (similar to loads) are used in the power balance equation (11).

10) Storage State of Charge:

$$SOC^S_{min,i} \le SOC^S_{i,t} \le SOC^S_{max,i} \quad \forall i \in \mathcal{S} \wedge t \in \mathcal{T}. \tag{20}$$

This constraint ensures that the storage SOC is always within acceptable range, considering the maximum allowed depth of discharge and the maximum capacity. Note that depending on the microgrid's operational conditions and storage technology, small violations from the lower bound of charge state are allowed; this can prevent undesired infeasibility of the microgrid generation scheduling problem arising from not respecting the lower limit of charge state. In this case, the lower bound of charge state in (20) is modified by defining the following soft constraint:

$$SOC^S_{i,t} \ge SOC^S_{min,i} - SOC^{S,slack}_{i,t}, \quad \forall i \in \mathcal{S} \wedge t \in \mathcal{T} \tag{21}$$

where non-negative slack variable $SOC^{S,slack}_{i,t}$ is penalized in the objective function. Thus, the penalty factor $C^{S,slack}_i$ is defined by adding $C^{S,slack}_i.SOC^{S,slack}_{i,t}$ to the objective function (10).

11) Storage Initial State:

$$SOC^S_{i,t} = SOC^S_{init,i} \quad \forall i \in \mathcal{S} \wedge t = 0 \tag{22}$$

where $SOC^S_{init,i}$ is provided by the storage local controller and is assumed to be within acceptable range.

12) Storage Energy Balance:

$$SOC^S_{i,t} - SOC^S_{i,t-1} + \left[\frac{P^{S,DHG}_{i,t}}{\eta^{S,DHG}_i} - \eta^{S,CHG}_i P^{S,CHG}_{i,t} + P^{S,loss}_i\right]\Delta T = 0. \quad \forall i \in \mathcal{S} \wedge t \in \mathcal{T} \tag{23}$$

This constraint dictates how storage SOC should be evolved over time, depending upon the storage charging and discharging powers, corresponding efficiencies, and standby loss. For a hydrogen storage system, $\eta^{S,CHG}_i$ and $\eta^{S,DHG}_i$ correspond to electrolyzer and fuel cell efficiencies, respectively. Also, since the dissipation of hydrogen is extremely low compared to other types of storage technologies, $P^{S,loss}_i$ can be neglected.

13) Storage Charging Power:

$$b^{S,CHG}_{i,t}.P^{S,CHG}_{min,i} \le P^{S,CHG}_{i,t} \le b^{S,CHG}_{i,t}.P^{S,CHG}_{max,i} \quad \forall i \in \mathcal{S} \wedge t \in \mathcal{T} \tag{24}$$

where $b^{S,CHG}_{i,t} = 1$ represents the online status of storage charging i (e.g., electrolyzer) at time step t. These complex constraints are required since particular types of storage devices (e.g., an electrolyzer in a hydrogen storage system) are not able to function below a certain level of electricity input power. Therefore, these constraints are enforced to model offline and online states as well as minimum and maximum power requirements in the online state. Note that an incentive ($I^{S,CHG}_i$) can be defined to promote storage charging if surplus power is available in the microgrid. In this case, the term $-I^{S,CHG}_i.P^{S,CHG}_{i,t}.\Delta T$ should be considered in the objective function (10).

14) Storage Charging Start-Up:

$$\delta^{S,CHG}_{i,t} - b^{S,CHG}_{i,t} + b^{S,CHG}_{i,t-1} \ge 0 \quad \forall i \in \mathcal{S} \wedge t \in \mathcal{T}. \tag{25}$$

Similar to the case of dispatchables, this constraint is enforced to model the start-up cost of storage charging i (e.g., electrolyzer).

15) Storage Discharging Power:

$$b^{S,DHG}_{i,t}.P^{S,DHG}_{min,i} \le P^{S,DHG}_{i,t} \le b^{S,DHG}_{i,t}.P^{S,DHG}_{max,i} \quad \forall i \in \mathcal{S} \wedge t \in \mathcal{T} \tag{26}$$

where $b^{S,DHG}_{i,t} = 1$ represents the online status of storage discharging i (e.g., fuel cell) at time step t. For a hydrogen storage

system, this constraint ensures that if a power contribution from the fuel cell is needed at time step t, its value should not be below or above certain limits. It is also important to note that the maximum discharging power in (26) is oftentimes constrained by the storage SOC. The storage local controller usually communicates this maximum discharging power with the microgrid control/energy management system; therefore, this value will be available in the generation scheduling routine at each time step.

16) Storage Discharging Start-Up:

$$\delta_{i,t}^{S,DHG} - b_{i,t}^{S,DHG} + b_{i,t-1}^{S,DHG} \geq 0 \quad \forall i \in \mathcal{S} \wedge t \in \mathcal{T}. \tag{27}$$

This constraint models the start-up cost of storage discharging i (e.g., fuel cell) in the objective function (10).

17) Storage Simultaneous Charging and Discharging:

$$b_{i,t}^{S,CHG} + b_{i,t}^{S,DHG} \leq 1 \quad \forall i \in \mathcal{S} \wedge t \in \mathcal{T}. \tag{28}$$

This constraint ensures that only charging or discharging will take place at any time step. For a hydrogen storage system, this constraint precludes simultaneous operation of electrolyzer and fuel cell.

18) Storage Charging MUT:

$$\begin{gathered} b_{i,t}^{S,CHG} - b_{i,t-1}^{S,CHG} - b_{i,k}^{S,CHG} \leq 0 \\ \forall i \in \mathcal{S} \wedge t \in \mathcal{T}^* \wedge k \in \mathcal{K}_3 \end{gathered} \tag{29}$$

where

$\mathcal{K}_3 = \{t, \ldots, min(t+10\times MUT_i^{S,CHG}-1, \text{prediction length})\}$.

19) Storage Charging MDT:

$$\begin{gathered} b_{i,t-1}^{S,CHG} - b_{i,t}^{S,CHG} + b_{i,k}^{S,CHG} \leq 1 \\ \forall i \in \mathcal{S} \wedge t \in \mathcal{T}^* \wedge k \in \mathcal{K}_4 \end{gathered} \tag{30}$$

where

$\mathcal{K}_4=\{t, \ldots, min(t + 10 \times MDT_i^{S,CHG}-1, \text{prediction length})\}$. Note that for a hydrogen storage system, abrupt start-up and shut-down causes damage to the electrolyzer due to shifts of temperature and pressure; therefore, (29) and (30) should be in place to increase the life cycle, physical integrity, and performance of the electrolyzer.

20) Storage Sustainability: If the storage device is supposed to be operated with a constant cycle over the prediction horizon, the following constraint can be enforced:

$$\begin{gathered} SOC_{i,t_1}^{S} = SOC_{i,t_2}^{S} \\ \forall i \in \mathcal{S} \wedge t_1 = 0 \wedge t_2 = \text{prediction length}. \end{gathered} \tag{31}$$

21) Storage Smooth Operation: Depending on the microgrid conditions and operational requirements of the storage devices, the following constraints can be considered to ensure smooth charging and discharging:

$$\begin{gathered} -\alpha_i^{S,CHG} \leq P_{i,t}^{S,CHG} - P_{i,t-1}^{S,CHG} \leq \alpha_i^{S,CHG} \\ -\beta_i^{S,DHG} \leq P_{i,t}^{S,DHG} - P_{i,t-1}^{S,DHG} \leq \beta_i^{S,DHG} \\ \forall i \in \mathcal{S} \wedge t \in \mathcal{T} \end{gathered} \tag{32}$$

where non-negative variables $\alpha_i^{S,CHG}$ and $\beta_i^{S,DHG}$ are penalized in the objective function. Thus, two penalty factors $C_i^{S,CHG}$ and $C_i^{S,DHG}$ are defined by adding $C_i^{S,CHG}.\alpha_i^{S,CHG}.\Delta T$ and $C_i^{S,DHG}.\beta_i^{S,DHG}.\Delta T$ in the objective function (10). These constraints limit the rates of change of storage charging and discharging powers. Note that the aforementioned smooth operation can also be achieved by the corresponding local controllers, depending on their design and implementation.

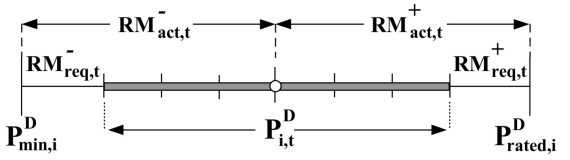

Fig. 2. Demonstration of a dispatchable's reserve power coverage.

V. Reserve Margins Considerations

Positive and negative reserve margins for the microgrid are considered to account for forecast errors or sudden increase/decrease in load and renewable powers so that load-generation balance can always be maintained. These positive and negative reserve margins are defined as a few percent of total loads and renewables as follows:

$$\begin{aligned} RM_{req,t}^{+} &= r^{+} \textstyle\sum_{i\in\mathcal{L}} P_{i,t}^{L} + u^{+} \sum_{i\in\mathcal{R}} P_{i,t}^{R} \\ RM_{req,t}^{-} &= r^{-} \textstyle\sum_{i\in\mathcal{L}} P_{i,t}^{L} + u^{-} \sum_{i\in\mathcal{R}} P_{i,t}^{R} \end{aligned} \tag{33}$$

where parameters r^{+}, r^{-}, u^{+}, and u^{-} are typically in the range of [0,0.2] which are set based on the microgrid conditions and requirements. As demonstrated in Fig. 2, while $RM_{req,t}^{+}$ and $RM_{req,t}^{-}$ are the minimum reserve margins required for the stable operation of a microgrid, the actual reserve margins ($RM_{act,t}^{+}$ and $RM_{act,t}^{-}$), which are realized in the microgrid, can be larger than $RM_{req,t}^{+}$ and $RM_{req,t}^{-}$, depending upon the operating power of the genset. However, the large values for $RM_{act,t}^{+}$ or $RM_{act,t}^{-}$ do not necessarily guarantee the stable operation of a microgrid. The speed of frequency recovery depends upon the type, number, and speed control mode of the generation units in a microgrid. Thus, with reference to Fig. 2, the maximum possible value of load step change that could be picked up by a single dispatchable genset is equal to $P_{rated,i}^{D} - P_{min,i}^{D}$; this value is typically around 50% of the genset's full-load capacity. Given the present technology and what is currently offered by most suppliers, the aforementioned load step change can, in fact, be picked up in one step. The frequency recovery time will depend on how fast the genset can raise its output power from 50% to 100% load in one step; it typically happens within a few seconds for a diesel genset with an isochronous speed control. However, multiple gensets running in ILS mode would have substantially better transient performance since each individual genset would only take up a portion of the substantial step load change.

With regard to Fig. 2, an undesired situation happens when the non-isochronous resources being commanded by the microgrid control or energy management system force the isochronous machine to approach its maximum/minimum limits. In this case, minimum required reserve margin is not maintained and the isochronous speed control, despite being fast, fails to control the frequency when faced with a big step load/renewable change. This is the reason that the steady-state power generation contribution of the isochronous machine and how it covers the reserve margins should be factored in the microgrid generation scheduling problem. The reserve margins

considerations are presented in this section for three types of dispatchables, renewables, and storage devices.

A. Dispatchables

As highlighted in Fig. 2, when a dispatchable provides the reserve margins defined by (33), its expected power contribution in the optimization routine will be placed in a tighter range. Therefore, the first implication of reserve power on the microgrid optimal generation scheduling is to change the upper and lower bounds of power in (12) for the dispatchable that provides the reserve margins (e.g., the isochronous machine). Thus, the following constraint can be applied for the single isochronous dispatchable i, which is forced to be online to cover the reserve margins requirements:

$$P^D_{min,i} + RM^-_{req,t} \le P^D_{i,t} \le P^D_{rated,i} - RM^+_{req,t} \quad \forall t \in \mathcal{T}. \tag{34}$$

Obviously, the above constraint is inadequate to model the operation of multiple dispatchables in ILS mode. Therefore, in order to accommodate a comprehensive scenario when a single or multiple dispatchables contribute to cover the reserve margins requirements, the following procedure is proposed.

Let $\mathcal{I}$ be the set of dispatchables running in ILS mode. This set is decided by the microgrid operator based on the system requirements and his/her knowledge of the generation and control system capabilities. The total actual reserve margins provided by those units belonging to set $\mathcal{I}$ and committed by the optimal generation scheduling problem should not fall below the minimum required reserve margins in the microgrid at any time step. These requirements can be enforced by the following constraints:

$$\sum_{\substack{i\in\mathcal{I}\\ b^D_{i,t}=1}} P^D_{rated,i} - \sum_{\substack{i\in\mathcal{I}\\ b^D_{i,t}=1}} P^D_{i,t} \ge RM^+_{req,t} \quad \forall t \in \mathcal{T} \tag{35}$$

$$\sum_{\substack{i\in\mathcal{I}\\ b^D_{i,t}=1}} P^D_{i,t} - \sum_{\substack{i\in\mathcal{I}\\ b^D_{i,t}=1}} P^D_{min,i} \ge RM^-_{req,t} \quad \forall t \in \mathcal{T}. \tag{36}$$

Incorporating the impact of binary variables $b^D_{i,t} = 1$ results in non-linear constraints. In order to keep the model in the framework of an MILP problem, new continuous variable $V^D_{i,t} = b^D_{i,t}.P^D_{i,t}$ is defined while considering additional constraints on this variable. Therefore, (35) and (36) are transformed to become the following constraints:

$$\sum_{i\in\mathcal{I}} b^D_{i,t}.P^D_{rated,i} - \sum_{i\in\mathcal{I}} V^D_{i,t} \ge RM^+_{req,t} \quad \forall t \in \mathcal{T} \tag{37}$$

$$\sum_{i\in\mathcal{I}} V^D_{i,t} - \sum_{i\in\mathcal{I}} b^D_{i,t}.P^D_{min,i} \ge RM^-_{req,t} \quad \forall t \in \mathcal{T} \tag{38}$$

$$b^D_{i,t}.P^D_{min,i} \le V^D_{i,t} \le b^D_{i,t}.P^D_{rated,i} \quad \forall i \in \mathcal{I} \wedge t \in \mathcal{T} \tag{39}$$

$$P^D_{i,t} - \left(1 - b^D_{i,t}\right) P^D_{rated,i} \le V^D_{i,t} \le P^D_{i,t} - \left(1 - b^D_{i,t}\right) P^D_{min,i} \quad \forall i \in \mathcal{I} \wedge t \in \mathcal{T}. \tag{40}$$

Constraints (39) and (40) are developed following the conventional procedure in order to remove non-linearity from the model [32], [33]. However, due to mutual impacts of binary variables $b^D_{i,t}$ and continuous variables $P^D_{i,t}$, an inherent difficulty with these constraints preclude them from adequately representing the behavior of the ILS operation. Thus, if $b^D_{i,t} = 0$ then for all $i \in \mathcal{I}$, $P^D_{i,t}$ also become zero and this makes the problem infeasible since (39) and (40) are transformed to $V^D_{i,t} = 0$ and $-P^D_{rated,i} \le V^D_{i,t} \le -P^D_{min,i}$ that should hold simultaneously for the non-negative continuous variables $V^D_{i,t}$. In order to address the aforementioned difficulty, the following constraint is proposed for consideration instead of constraint (40):

$$P^D_{i,t} - \left(1 - b^D_{i,t}\right) P^D_{rated,i} \le V^D_{i,t} \le P^D_{i,t} + \left(1 - b^D_{i,t}\right) P^D_{rated,i} \quad \forall i \in \mathcal{I} \wedge t \in \mathcal{T}. \tag{41}$$

The proposed change includes modifying the upper bound of $V^D_{i,t}$ in constraint (40).

Based on the philosophy of ILS operation discussed in Section II-B, each machine shares an equal percentage of its nameplate rating power at any time step; this is reflected in (2). Therefore, the following constraint also governs the power generation of committed gensets in this mode of operation:

$$P^D_{j,t}.\sum_{\substack{i\in\mathcal{I}\\ b^D_{i,t}=1}} P^D_{rated,i} - P^D_{rated,j}.\sum_{\substack{i\in\mathcal{I}\\ b^D_{i,t}=1}} P^D_{i,t} = 0 \quad \forall j \in \mathcal{I} \wedge t \in \mathcal{T} \wedge b^D_{j,t} = 1. \tag{42}$$

Incorporating the impact of binary variables $b^D_{i,t}$ and $b^D_{j,t}$ results in

$$b^D_{j,t}.P^D_{j,t}.\sum_{i\in\mathcal{I}} b^D_{i,t}.P^D_{rated,i} - P^D_{rated,j}.b^D_{j,t}.\sum_{i\in\mathcal{I}} b^D_{i,t}.P^D_{i,t} = 0 \quad \forall j \in \mathcal{I} \wedge t \in \mathcal{T} \tag{43}$$

which can then be summarized in the following constraint by considering the previously-defined variable $V^D_{i,t}$:

$$\sum_{i\in\mathcal{I}} b^D_{i,t}.V^D_{j,t}.P^D_{rated,i} - P^D_{rated,j}.\sum_{i\in\mathcal{I}} b^D_{j,t}.V^D_{i,t} = 0 \quad \forall j \in \mathcal{I} \wedge t \in \mathcal{T}. \tag{44}$$

Again, in order to remove non-linearity from the model, a new continuous auxiliary variable $W^D_{i,j,t} = b^D_{i,t}.V^D_{j,t}$ is defined by considering additional constraints on this variable. Therefore, (42) is transformed into the following set of constraints:

$$\sum_{i\in\mathcal{I}} W^D_{i,j,t}.P^D_{rated,i} - P^D_{rated,j}\sum_{i\in\mathcal{I}} W^D_{j,i,t} = 0 \quad \forall j \in \mathcal{I} \wedge t \in \mathcal{T} \tag{45}$$

$$0 \le W^D_{i,j,t} \le b^D_{i,t}.P^D_{rated,j} \quad \forall i,j \in \mathcal{I} \wedge t \in \mathcal{T} \tag{46}$$

$$V^D_{j,t} - \left(1 - b^D_{i,t}\right) P^D_{rated,j} \le W^D_{i,j,t} \le V^D_{j,t} + \left(1 - b^D_{i,t}\right) P^D_{rated,j} \quad \forall i,j \in \mathcal{I} \wedge t \in \mathcal{T}. \tag{47}$$

Therefore, the combination of constraints (37)–(39), (41), (45)–(47) models the ILS operation of multiple dispatchable gensets in the microgrid optimal generation scheduling problem.

B. Renewables

Power constraints of renewable sources are represented as follows:

$$P^R_{i,t} = P^{R_f}_{i,t} \quad \forall i \in \mathcal{R} \wedge t \in \mathcal{T} \tag{48}$$

where $P^{R_f}_{i,t}$ is the forecasted value of renewable power source i at time step t. This constraint ensures that only the forecasted

values of renewable power sources (similar to loads) are used in the power balance equation [i.e., (11)].

In order to support the isochronous operation of a low-intermittent renewable power source (e.g., a run-of-the-river hydro unit with reservoir) in the microgrid optimal generation scheduling problem, the following procedure is proposed.

The renewable power $P^R_{i,t}$ in the power balance constraint (11) will no longer be a parameter that can take forecasted values. Therefore, (48) should be relaxed, and $P^R_{i,t}$ will be treated as a decision variable in the optimal generation scheduling problem. However, its upper and lower bounds should be adjusted similar to (34) to respect the reserve margins requirements.

Although a renewable power source such as a run-of-the-river hydro unit with reservoir can have the capability of running in isochronous mode, it nevertheless has a limited degree of intermittency and fluctuation during certain times. In that respect, it is different from a dispatchable resource, which has a fixed output power. The consequence of this behavior on the microgrid generation scheduling problem is that the renewable generation unit may not always be able to generate the power level resulting from the optimization problem; this leads to load-generation imbalance or lack of adequate reserve margin. In order to address this problem, a parameter entitled renewable capability ($C^R_{i,t}$) is defined which will be multiplied by the upper bound of renewable power [34]. This is a parameter between 0 and 1, and decided based on meteorological observation data. Therefore, for a low-intermittent renewable power source i operating in isochronous mode, the following constraint will be applied:

$$\left(P^R_{min,i}+RM^-_{req,t}\right) \le P^R_{i,t} \le \left(C^R_{i,t}.P^R_{rated,i}-RM^+_{req,t}\right) \quad \forall t \in \mathcal{T}. \tag{49}$$

In fact, the risk of infeasibility is mitigated by reflecting the forecasted level of intermittency in this constraint.

The presumption in the proposed procedure is that the renewable capabilities are correctly decided for the entire prediction horizon; however, erroneous values may lower the reserve margins or render the optimization problem infeasible by deteriorating the generation-load balance. In order to address the prediction errors, a slack variable ($P^{sys,slack}_t$) is proposed to be added to the power balance (11). A sufficiently large penalty factor ($C^{sys,slack}_t$) is then defined to penalize the proposed slack variable in the objective function. Therefore, the suggested procedure is finalized by adding the term $C^{sys,slack}_t.P^{sys,slack}_t.\Delta T$ to the objective function.

C. Storage Devices

Depending upon the microgrid conditions, particular types of storage devices that are equipped with appropriate bi-directional power conversion systems can cover the microgrid reserve margin requirements. Therefore, similar constraints to those of dispatchables in Section V-A can be employed in order to support this feature in the microgrid optimal generation scheduling framework. This includes modifying the lower and upper bounds of both charging and discharging powers since reserve margins should be covered in either charging or discharging states. However, appropriate constraints are in place to ensure that only charging or discharging will take place at any time step. It is worth mentioning that the proposed approach does not consider the scenario in which a combination of dispatchable and storage devices operate in ILS mode; this arrangement is uncommon in actual practice due to the different dynamic behaviors.

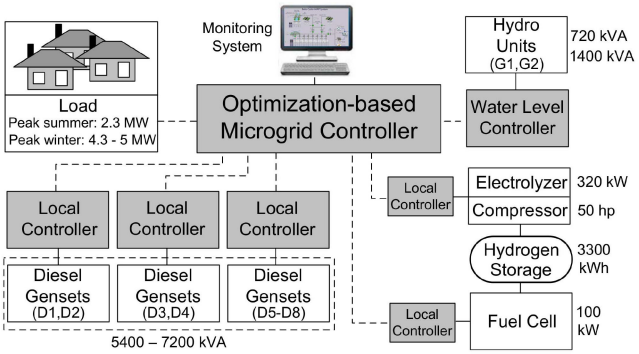

Fig. 3. Bella Coola microgrid system configuration.

VI. Real-World Microgrid Example

In order to represent the proposed frequency regulation considerations in the microgrid optimal generation scheduling problem, the real-world microgrid example of Bella Coola in the North of British Columbia, Canada, is selected. The Bella Coola system configuration and its corresponding key information are shown in Fig. 3, where there are six to eight diesel gensets, two run-of-the-river hydro units, and one hydrogen-based storage system composed of an alkaline electrolyzer, high-pressure hydrogen cylinders, and an air cooled proton exchange membrane fuel cell [22]. Moreover, both hydro and diesel gensets in this microgrid have the capability of operating in isochronous speed control mode. Thus, in winter, all running diesel gensets are usually operated in ILS mode in order to accommodate considerable load variation during 24 h and to maintain enough spinning reserve at all times. However, during non-winter months starting from April–May to late November, the larger hydro unit is operated in isochronous mode due to the significant contribution of hydro units and in order to minimize the operation of costly and polluting diesel gensets.

VII. Numerical Illustration

The optimal generation scheduling problem with the proposed reserve power considerations was modeled in AMPL [35] and solved using CPLEX [36], on an IBM eServer xSeries 460 with 8 Intel Xeon 2.8 GHz processors and 3 GB (effective) of RAM. The model's complete data has been provided in [37]; however, some major parameters corresponding to diesel gensets and hydrogen storage system are reflected in Tables I and II, respectively. Three scenarios with different type/number of isochronous units are considered in this section. The first scenario corresponds to a typical summer day with the total costs (start-up and operation) of $1923, while the second and third scenarios represent the Bella Coola microgrid operation on a typical winter day with the total costs of

TABLE I
DIESEL GENSETS PARAMETERS

		D1	D2	D3	D4	D5	D6	D7
$P^D_{rated,i}$	kW	1000	800	1000	300	300	1000	1000
$P^D_{min,i}$	kW	400	320	400	120	120	400	400
$\eta^D_{rated,i}$	kWh/kg	4.74	4.57	4.74	4.41	4.41	4.74	4.74
$\eta^D_{min,i}$	kWh/kg	4.54	4.45	4.54	4.32	4.32	4.54	4.54
LF^D_i	-	0.7	0.7	0.7	0.7	0.7	0.7	0.7
Cst^D_i	$	100	80	100	30	30	100	100
Csh^D_i	$	100	80	100	30	30	100	100
MUT^D_i	hour	3	3	3	1	1	3	3
MDT^D_i	hour	1	1	1	0.5	0.5	1	1
RU^D_i	kW/step	120	120	120	120	120	120	120
RD^D_i	kW/step	120	120	120	120	120	120	120

TABLE II
HYDROGEN STORAGE SYSTEM PARAMETERS

Storage Charging (Electrolyzer)			Storage Discharging (Fuel Cell)		
$P^{S,CHG}_{max,i}$	kW	320	$P^{S,DHG}_{max,i}$	kW	100
$P^{S,CHG}_{min,i}$	kW	120	$P^{S,DHG}_{min,i}$	kW	10
$\eta^{S,CHG}_i$	%	65	$\eta^{S,DHG}_i$	%	48
$MUT^{S,CHG}_i$	hour	3	$Cop^{S,DHG}_i$	$/kWh	0.05
$MDT^{S,CHG}_i$	hour	1	$Cst^{S,DHG}_i$	$	100
$Cop^{S,CHG}_i$	$/kWh	0.05			
$Cst^{S,CHG}_i$	$	100			
Hydrogen Cylinders					
$SOC^S_{max,i}$	kWh	3300	$SOC^S_{init,i}$	kWh	800 (summer)
$SOC^S_{min,i}$	kWh	500	$SOC^S_{init,i}$	kWh	1650 (winter)
$P^{S,loss}_i$	kWh/h	0			

$20 120 and $20 416, respectively. These larger costs are due to the significant share of diesel gensets required to cover the high electricity demand during winter. It is also important to note that the optimality gap in CPLEX (i.e., `mipgap`) was set to be equal to 0.005. Therefore, all the reported results are within 0.5% of optimality. Furthermore, the following directives were used to improve the CPLEX computation time performance: `startalgorithm`=6 and `varsel`=3 [36]. Based on the aforementioned settings, all the results were obtained within reasonable times of less than dispatch time (i.e., 12 min).

A. Scenario I: Hydro in Isochronous Speed Control Mode

Optimal power contributions of different devices in this scenario are shown in Fig. 4 with the scale of *x*-axis being changed from time step (1–120) to hour (1–24) for greater readability. This figure reflects the dominant share of hydro units; however, only one diesel (no. 5) is required for a duration of almost 5.5 h to cover the peak demand. It is important to note that the renewable power source is not only able to cover the reserve power requirements but also to run the electrolyzer that stores hydrogen during off-peak hours to partially offset diesel use later during on-peak hours. Observe in Fig. 4 that, the 3-h MUT requirement for electrolyzer is also respected.

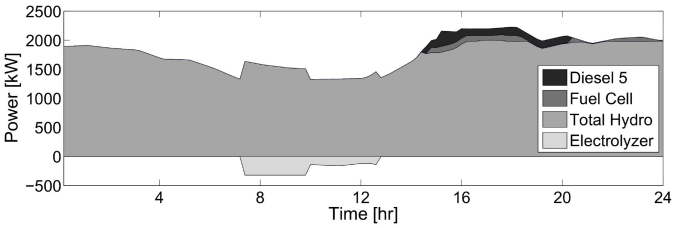

Fig. 4. Optimal power contribution of generation and storage devices for scenario I (summertime): hydro (G2) in isochronous speed control mode.

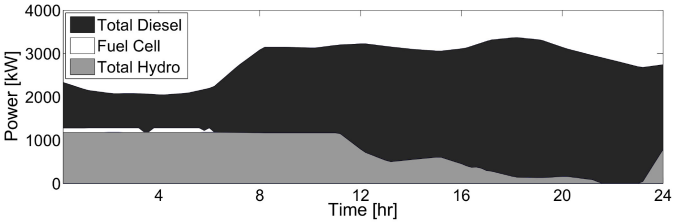

Fig. 5. Optimal power contribution of generation and storage devices for scenario II (wintertime): all diesel gensets in ILS mode.

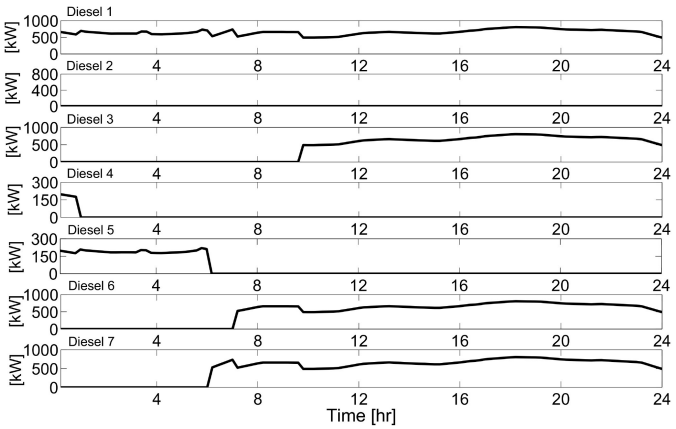

Fig. 6. Diesel gensets' optimal output power for scenario II (wintertime): all diesel gensets in ILS mode.

B. Scenario II: All Diesel Gensets in ILS Mode

This scenario represents the typical operation practice in Bella Coola during wintertime with the dominant share of diesel gensets as depicted in Fig. 5. Observe that diesel is offset by fuel cell operation during the first 6 h, and this phenomenon can be explained by the initial value of the hydrogen SOC.

Optimal output power of diesel gensets in this scenario is shown in Fig. 6. Despite having all units set in ILS mode, diesel genset 2 is not committed by the generation scheduling problem. Therefore, all units in ILS mode are not forced to be online. The reason behind not having genset 2 committed is that it has the second lowest efficiency (i.e., 4.57 kWh/kg or 36.72%) at rated power. Diesel gensets 4 and 5 are both committed for the first hour despite having the lowest efficiencies (4.41 kWh/kg or 35.44%) at rated powers. They are used due to their lowest start-up costs (38% less than that of genset 2). The other contributing factors are the high acceptable minimum power (320 kW) and 3-h MUT

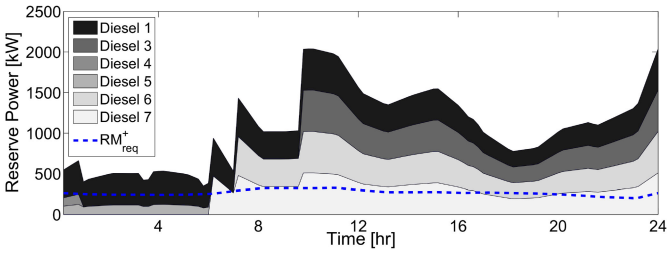

Fig. 7. Minimum required positive reserve power (RM^{+}_{req}) and contribution of multiple diesel gensets to actual positive reserve power for scenario II.

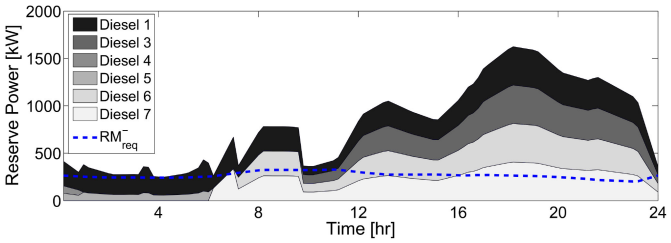

Fig. 8. Minimum required negative reserve power (RM^{-}_{req}) and contribution of multiple diesel gensets to actual negative reserve power for scenario II.

requirements of genset 2 which would both result in excess power in the microgrid. Also, note that the 1-h MUT requirement for gensets 4 and 5 and the 3-h MUT requirement for all remaining units are respected. Observe that diesel gensets are started at different times but once they become online, they properly share load with other isochronous units by following a similar pattern since they share an equal percentage of their rated powers. Fig. 7 outlines the minimum required (dotted line) and actual reserve powers along with share of multiple diesel gensets for positive margin. The same format is used in Fig. 8, except that it shows the negative margin. Observe in these figures that the minimum requirements of both positive and negative reserve margins are satisfied. For the first 6 h, the contribution of the isochronous units to actual reserve power are different due to the operation of dissimilar gensets but for the remaining hours the share of online isochronous units are similar since they all have equal 1000 kW rated powers.

C. Scenario III: Diesel Gensets 2, 6, and 7 in ILS Mode

Optimal output power of diesel gensets in this scenario is shown in Fig. 9. Observe in this figure that diesel genset 1 is also committed for the entire prediction horizon; thus, committed units can be in the pool of non-isochronous units, depending upon the load and renewable powers. Note that this unit is also permitted to reach its rated power at times since it does not contribute to reserve power coverage. The minimum requirement and actual reserve powers depicting the share of diesel gensets 2, 6, and 7 for positive and negative margins, respectively, are shown in Figs. 10 and 11. These figures confirm that the minimum requirements of reserve powers are also met in this scenario; however, similar to the previous scenario, a different number of units contribute to reserve power in different time frames. Thus, diesel genset 7 is the only contributor to reserve power for the first 6.4 h; diesel gensets 6 and 7 contribute equally to reserve power between 6.4 and

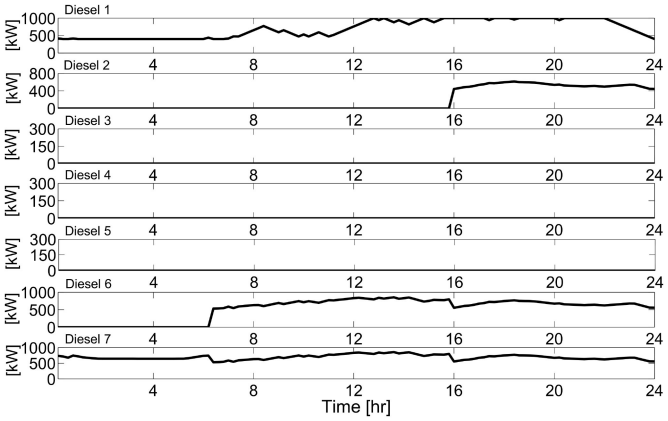

Fig. 9. Diesel gensets' optimal output power for scenario III (wintertime): diesel gensets 2, 6, and 7 in ILS mode.

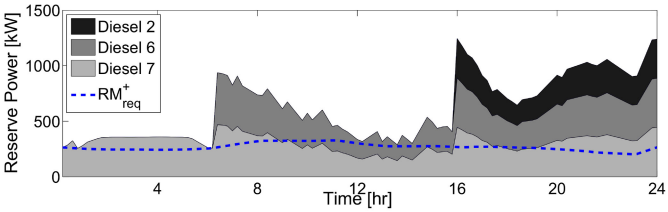

Fig. 10. Minimum required positive reserve power (RM^{+}_{req}) and contribution of multiple diesel gensets to actual positive reserve power for scenario III.

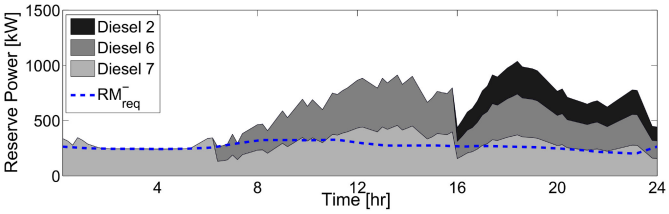

Fig. 11. Minimum required negative reserve power (RM^{-}_{req}) and contribution of multiple diesel gensets to actual negative reserve power for scenario III.

16 h as justified by their equal ratings. For the remainder of the prediction horizon all the isochronous units contribute to reserve power. The relatively lower kW contribution of diesel genset 2 can be explained by its lower power rating (800 kW) compared to 1000-kW of units 6 and 7.

It is worth mentioning that any desired number of dispatchables (e.g., diesel gensets) set to operate in ILS mode, especially in the microgrids with relatively higher levels of required reserve margin, will not necessarily result in appropriate outcomes. This is mostly because of the dispatchables' minimum power requirement, which is typically around 40–50% of their rated powers. This relatively high level of minimum power leaves a limited range for each individual isochronous unit to contribute its share of positive and negative reserve margins. Therefore, numerical and/or operational difficulties are expected when limited number of units are set to cover relatively large reserve margins. Thus, setting such dispatchables in ILS mode indirectly forces them to share higher percentages of their full-load capacity to respect the minimum reserve power requirement. The consequence of this behavior results in excess power, which is consumed to charge the

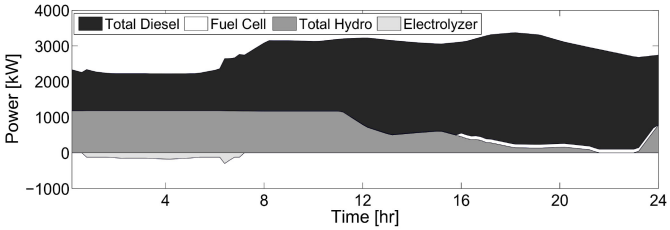

Fig. 12. Optimal power contribution of generation and storage devices for scenario III (wintertime): diesel gensets 2, 6, and 7 in ILS mode.

storage devices in the microgrid; storing energy based on a non-renewable power source may be an undesired operational practice. This is illustrated in Fig. 12 for scenario III, where the electrolyzer is operated for almost 6 h. Furthermore, this excess power is sometimes beyond the level that can even be absorbed by the storage devices, causing an infeasibility of the optimization problem. In view of all these considerations, a sufficient number of units should be set in ILS mode to ensure both feasibility and operational acceptability.

VIII. Conclusion

This paper examined the frequency control considerations of microgrids within the framework of the optimal generation scheduling problem. Inspired by practical microgrid applications, different methods to control frequency were discussed. Based on the operational limitations experienced in real-world microgrid projects, a comprehensive optimal generation scheduling problem was formulated. This formulation was extended by proposing and developing appropriate constraints to model different types of frequency-control mechanisms. Finally, the usefulness of the proposed model was demonstrated by applying it to the real-case of the Bella Coola microgrid in British Columbia, Canada.

Acknowledgment

The authors would like to thank G. Olson from kW Rx, LLC, for his valuable comments and helpful discussions.

References

[1] R. H. Lasseter and P. Piagi, "Microgrid: A conceptual solution," in *Proc. IEEE 35th Annu. Power Electron. Spec. Conf. (PESC)*, Aachen, Germany, 2004, pp. 4285–4290.

[2] G. Venkataramanan and C. Marnay, "A larger role for microgrids," *IEEE Power Energy Mag.*, vol. 6, no. 3, pp. 78–82, May/Jun. 2008.

[3] (Sep. 15, 2010). Aboriginal Affairs and Northern Development Canada. *Aboriginal and Northern Off-Grid Communities*. [Online]. Available: http://www.aadnc-aandc.gc.ca/eng/1314295992771/1314296121126#comm

[4] D. Cornforth, "The role of microgrids in the smart grid," *J. Electron. Sci. Technol.*, vol. 9, no. 1, pp. 9–16, Mar. 2011.

[5] J. Wang, A. Botterud, V. Miranda, C. Monteiro, and G. Sheble, "Impact of wind power forecasting on unit commitment and dispatch," in *Proc. 8th Int. Workshop Large-Scale Integr. Wind Power Power Syst.*, Bremen, Germany, Oct. 2009, pp. 1–8.

[6] J. Wang *et al.*, "Representing wind power forecasting uncertainty in unit commitment," *Appl. Energy*, vol. 88, no. 11, pp. 4014–4023, Nov. 2011.

[7] S. J. Wang, S. M. Shahidehpour, D. S. Kirschen, S. Mokhtari, and G. D. Irisarri, "Short-term generation scheduling with transmission and environmental constraints using an augmented Lagrangian relaxation," *IEEE Trans. Power Syst.*, vol. 10, no. 3, pp. 1294–1301, Aug. 1995.

[8] M. P. Nowak and W. Römisch, "Stochastic Lagrangian relaxation applied to power scheduling in a hydro-thermal system under uncertainty," *Ann. Oper. Res.*, vol. 100, nos. 1–4, pp. 251–272, Dec. 2000.

[9] M. Carrion and J. M. Arroyo, "A computationally efficient mixed-integer linear formulation for the thermal unit commitment problem," *IEEE Trans. Power Syst.*, vol. 21, no. 3, pp. 1371–1378, Aug. 2006.

[10] M. M. Hadji and B. Vahidi, "A solution to the unit commitment problem using imperialistic competition algorithm," *IEEE Trans. Power Syst.*, vol. 27, no. 1, pp. 117–124, Feb. 2012.

[11] T. Logenthiran and D. Srinivasan, "Short term generation scheduling of a microgrid," in *Proc. IEEE Reg. TENCON Conf.*, Singapore, Jan. 2009, pp. 1–6.

[12] A. M. Zein Alabedin, E. F. El-Saddany, and M. M. A. Salama, "Generation scheduling in microgrids under uncertainties in power generation," in *Proc. IEEE Electr. Power Energy Conf. (EPEC)*, London, ON, Canada, Oct. 2012, pp. 133–138.

[13] N. Hatziargyriou *et al.*, "Energy management and control of island power systems with increased penetration from renewable sources," in *Proc. IEEE Power Energy Soc. Win. Meeting*, vol. 1. New York, NY, USA, 2002, pp. 335–339.

[14] C. A. Hernandez-Aramburo, T. C. Green, and N. Mugniot, "Fuel consumption minimization of a microgrid," *IEEE Trans. Ind. Appl.*, vol. 41, no. 3, pp. 673–681, May/Jun. 2005.

[15] F. A. Mohamed and H. N. Koivo, "System modelling and online optimal management of microgrid using mesh adaptive direct search," *Int. J. Elect. Power Energy Syst.*, vol. 32, no. 5, pp. 398–407, Dec. 2010.

[16] A. G. Tsikalakis and N. D. Hatziargyriou, "Centralized control for optimizing microgrid operation," in *Proc. IEEE Power Energy Soc. Gen. Meeting*, San Diego, CA, USA, Jul. 2011, pp. 1–8.

[17] C. Chen, S. Duan, T. Cai, B. Liu, and G. Hu, "Smart energy management system for optimal microgrid economic operation," *IET Renew. Power Gener.*, vol. 5, no. 3, pp. 258–267, May 2011.

[18] S. J. Ahn and S. I. Moon, "Economic scheduling of distributed generators in a microgrid considering various constraints," in *Proc. IEEE Power Energy Soc. Gen. Meeting*, Calgary, AB, Canada, Jul. 2009, pp. 1–6.

[19] Y. C. Wu, M. J. Chen, J. Y. Lin, W. S. Chen, and W. L. Huang, "Corrective economic dispatch in a microgrid," *Int. J. Numer. Model. Electron. Netw. Devices Fields*, vol. 26, pp. 140–150, Jun. 2012.

[20] X. Wu, X. Wang, and Z. Bie, "Optimal generation scheduling of a microgrid," in *Proc. 3rd IEEE PES Innov. Smart Grid Technol. (ISGT Europe)*, Berlin, Germany, Oct. 2012, pp. 1–7.

[21] C. I. Hubert, *Electric Machines: Theory, Operation, Applications, Adjustment, and Control*, 2nd ed. Upper Saddle River, NJ, USA: Prentice Hall, 2002.

[22] A. H. Hajimiragha and M. R. Dadash Zadeh, "Research and development of a microgrid control and monitoring system for the remote community of Bella Coola: Challenges, solutions, achievements and lessons learned," in *Proc. IEEE Int. Conf. Smart Energy Grid Eng. (SEGE)*, Oshawa, ON, Canada, Aug. 2013, pp. 1–6.

[23] G. Olson. (2010). *White paper on paralleling dissimilar generators: Part 3-load sharing compatibility*, Cummins Power Generation. [Online]. Available: http://www.cumminspower.com/www/literature/technicalpapers/PT-9017-P3-Dissimilar-en.pdf

[24] M. B. Delghavi and A. Yazdani, "Islanded-mode control of electronically coupled distributed-resource units under unbalanced and nonlinear load conditions," *IEEE Trans. Power Del.*, vol. 26, no. 2, pp. 661–673, Apr. 2011.

[25] A. Yazdani and R. Iravani, *Voltage-Sourced Converters in Power Systems*. Piscataway, NJ, USA: Wiley, Feb. 2010.

[26] K. T. Tan, P. L. So, Y. C. Chu, and M. Z. Q. Chen, "Coordinated control and energy management of distributed generation inverters in a microgrid," *IEEE Trans. Power Del.*, vol. 28, no. 2, pp. 704–713, Apr. 2013.

[27] E. F. Camacho and C. Bordons, *Model Predictive Control*, 2nd ed. Berlin, Germany: Springer-Verlag, 2002.

[28] L. Xie and M. D. Ilic, "Model predictive dispatch in electric energy systems with intermittent resources," in *Proc. IEEE Int. Conf. Syst. Man Cybern.*, Singapore, Oct. 2008, pp. 42–47.

[29] J. M. Arroyo and A. J. Conejo, "Optimal response of a thermal unit to an electricity spot market," *IEEE Trans. Power Syst.*, vol. 15, no. 3, pp. 1098–1104, Aug. 2000.

[30] J. M. Arroyo and A. J. Conejo, "Modeling of start-up and shut-down power trajectories of thermal units," *IEEE Trans. Power Syst.*, vol. 3, no. 19, pp. 1562–1568, Aug. 2004.

[31] S. Takriti and J. R. Birge, "Using integer programming to refine Lagrangian-based unit commitment solutions," *IEEE Trans. Power Syst.*, vol. 15, no. 1, pp. 151–156, Feb. 2000.

[32] C. A. Floudas, *Nonlinear and Mixed-Integer Programming—Fundamentals and Applications*. Oxford, U.K.: Oxford Univ. Press, 1995.
[33] H. P. Williams, *Model Building in Mathematical Programming*. Hoboken, NJ, USA: Wiley, 2013.
[34] M. R. Dadash Zadeh, A. H. Hajimiragha, and M. J. Krok, "Optimization of microgrid including renewable power source," U.S. Patent 2013/0 190 938 A1, Jul. 25, 2013.
[35] R. Fourer, D. M. Gay, and B. W. Kernighan, *AMPL: A Modeling Language for Mathematical Programming*, 2nd ed. Pacific Grove, CA, USA: Duxbury Press, 2002.
[36] *IBM ILOG AMPL Version 12.1 User's Guide*, IBM Corp., Armonk, NY, USA, Jun. 2009.
[37] A. H. Hajimiragha, M. R. Dadash Zadeh, and S. Moazeni. (Sep. 2014). *Microgrid Data*. [Online]. Available: http://www.eng.uwo.ca/people/mdadash/mgdata.pdf

Amir H. Hajimiragha (S'09–M'10–SM'13) received the B.Sc. degree from the K. N. Toosi University of Technology, Tehran, Iran; the M.Sc. degree from the Royal Institute of Technology, Stockholm, Sweden; and the Ph.D. degree from the University of Waterloo, Waterloo, ON, Canada, in 1995, 2005, and 2010, respectively, all in electrical engineering.

He began his career in 1996 as a research engineer at the Electric Power Research Center, Tehran, where he researched flicker assessment of alloy steel plants. Between 1998 and 2003, he was at Niroo Research Institute, Tehran, in different research and managerial positions, including the fields of power quality, energy management, power plants, and scientific publishing. Prior to joining General Electric (GE) in 2010, he worked as a Post-Doctoral Researcher at the University of Waterloo, where he investigated the grid impacts of fuel cell and plug-in hybrid electric vehicles. Currently, he is a Lead Application Engineer at the General Electric GridIQ Innovation Center, Markham, ON, where he is involved in research and development, and new product introduction programs concerning microgrids and distribution systems automation. His current research interests include the areas of integrated energy systems, hydrogen economy, microgrids, grid impacts of alternative-fuel vehicles, and smart grids.

Dr. Hajimiragha was the recipient of several national and international awards, including the 2011 Institute of Engineering and Technology International Innovation Award in the category of Built Environment, the 2008 Mathematics of Information Technology and Complex Systems National Award in the Category of Best Novel Use of Mathematics in Technology Transfer, and the 2008 University of Waterloo Exceptional Teaching Award.

Mohammad R. Dadash Zadeh (M'06–SM'14) received the B.Sc. and M.Sc. degrees from the University of Tehran, Tehran, Iran, in 2002 and 2005, respectively, and the Ph.D. degree from the University of Western Ontario, London, ON, Canada, in 2009, all in electrical engineering.

From 2002 to 2005, he was with Moshanir Power Engineering Consultants in Tehran, Iran, as a System Study Engineer. From 2009 to 2010, he was a Post-Doctoral Fellow at the University of Western Ontario. From 2010 to 2011, he was with General Electric Multilin, Markham, ON. Since 2011, he has been an Assistant Professor with the Electrical and Computer Engineering Department, University of Western Ontario. His current research interests include power system protection, control, and analysis.

Somayeh Moazeni (M'13) received the B.Sc. and M.Sc. degrees in mathematics from Tehran Polytechnic, Tehran, Iran, in 2004 and 2005, respectively, and the MMATH and Ph.D. degrees in combinatorics and optimization and in computer science from the University of Waterloo, Waterloo, ON, Canada, in 2006 and 2011, respectively.

She is currently an Assistant Professor with the School of Systems and Enterprises, Stevens Institute of Technology, Hoboken, NJ, USA. Her current research interests include numerical optimization; optimization under uncertainty, especially stochastic optimization and robust optimization; risk management; and financial optimization.

Dr. Moazeni was the recipient of several national and international awards, including the 2009 Google Canada Anita Borg Memorial Scholarship, and the 2013 Natural Sciences and Engineering Research Council of Canada Post-Doctoral Fellowship.